11.4 Voltage Stability

Yakout Mansour and Claudio Cañizares

Voltage stability "refers to the ability of a power system to maintain steady voltages at all buses in the system after being subjected to a disturbance from a given initial operating condition" (IEEE-CIGRE, 2004). If voltage stability exists, the voltage and power of the system will be controllable at all times. In general, the inability of the system to supply the required demand leads to a voltage instability (voltage collapse).

The nature of voltage instability phenomena can be either fast (short-term, with voltage collapse in the order of fractions of a second to a few seconds) or slow (long-term, with voltage collapse in minutes to hours) (IEEE-CIGRE, 2004). Short-term voltage stability problems are usually associated with the rapid response of voltage controllers (e.g. generators' AVR) and power electronic converters, such as those encountered in Flexible AC Transmission System or FACTS controllers and HVDC links. In the case of voltage regulators, voltage instability is usually related to inappropriate tuning of the system controllers. Voltage stability in converters, on the other hand, is associated with commutation issues in the electronic switches that make up the converters, particularly when these converters are connected to "weak" ac systems, i.e. systems with poor reactive power support. These fast voltage stability problems have been studied using a variety of analysis techniques and tools that properly model and simulate the dynamic response of the voltage controllers and converters under study, such as transient stability programs and electromagnetic transient simulators. This chapter does not discuss these particular issues, concentrating rather on a detailed presentation of long-term voltage instability phenomena in power systems.

Basic Concepts

Voltage instability of radial distribution systems has been well recognized and understood for decades (Venikov, 1970; 1980) and was often referred to as load instability. Large interconnected power networks did not face the phenomenon until late 1970s and early 1980s.

Most of the early developments of the major HV and EHV networks and interties faced the classical machine angle stability problem. Innovations in both analytical techniques and stabilizing measures made it possible to maximize the power transfer capabilities of the transmission systems. The result was increasing transfers of power over long distances of transmission. As the power transfer increased, even when angle stability was not a limiting factor, many utilities have been facing a shortage of voltage support. The result ranged from post contingency operation under reduced voltage profile to total voltage collapse. Major outages attributed to this problem have been experienced in the northeastern part of the U.S., France, Sweden, Belgium, Japan, along with other localized cases of voltage collapse (Mansour, 1990; US-Canada, 2004). Accordingly, voltage stability has imposed itself as a governing factor in both planning and operating criteria of a number of utilities. Consequently, sound analytical procedures, quantitative measures of proximity to voltage instability have been developed for the past two decades.

Generator-Load Example

The simple generator-load model depicted in Fig. 11.12 can be used to readily explain the basic concepts behind voltage stability phenomena. The power flow model of this system can be represented by the following equations:

$$0 = P_L - \frac{V_1 V_2}{X_L} \sin\delta$$

$$0 = kP_L + \frac{V_2^2}{X_L} - \frac{V_1 V_2}{X_L} \cos\delta$$

$$0 = Q_G - \frac{V_1^2}{X_L} + \frac{V_1 V_2}{X_L} \cos\delta$$

where $\delta = \delta_2 - \delta_1$, $P_G = P_L$ (no losses), $Q_L = k\,P_L$ (constant power factor load).

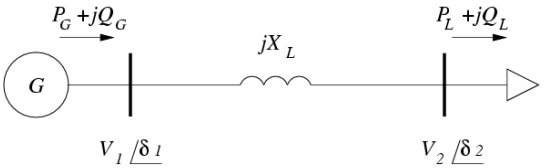

FIGURE 11.12 Generator-load example.

All solutions to these power flow equations, as the system load level P_L is increased, can be plotted to yield PV curves (bus voltage versus active power load levels) or QV curves (bus voltage versus reactive power load levels) for this system. For example, Fig. 11.13 depicts the PV curves at the load bus obtained from these equations for $k = 0.25$ and $V_1 = 1$ p.u. when generator limits are neglected, and for two values of X_L to simulate a transmission system outage or contingency by increasing its value. Figure 11.14 depicts the power flow solution when reactive power limits are considered, for $Q_{Gmax} = 0.5$ and $Q_{Gmin} = -0.5$. Notice that these PV curves can be readily transformed into QV curves by properly scaling the horizontal axis.

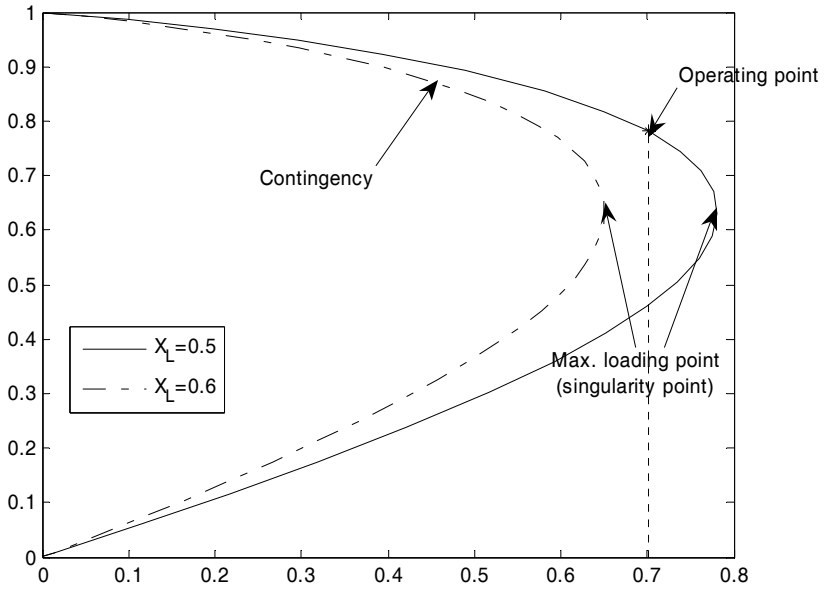

FIGURE 11.13 PV curve for generator-load example without generator reactive power limits.

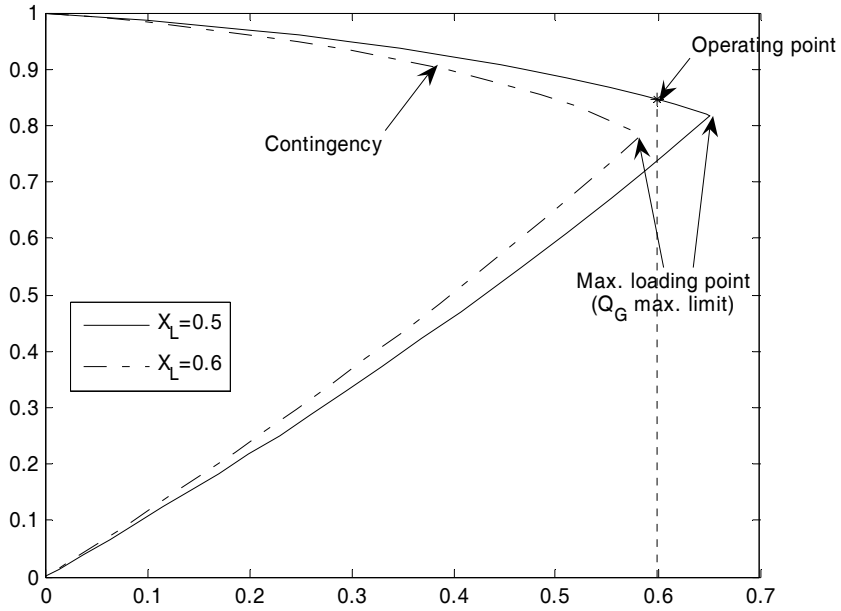

FIGURE 11.14 PV curve for generator-load example considering generator reactive power limits.

In Fig. 11.13, the maximum loading corresponds to a singularity of the Jacobian of the power flow equations, and may be associated with a *saddle-node bifurcation* of a dynamic model of this system (Cañizares, 2002). (A saddle-node bifurcation is defined in

a power-flow model of the power grid, which is considered a nonlinear system, as a point at which 2 power-flow solutions merge and disappear as typically the load, which is a system parameter, is increased; the Jacobian of the power-flow equations become singular at this "bifurcation" or "merging" point.) Observe that if the system were operating at a load level of P_L = 0.7 p.u., the contingency would basically result in the disappearance of an operating point (power flow solution), thus leading to a voltage collapse.

Similarly, if there is an attempt to increase P_L (Q_L) beyond its maximum values in Fig. 11.14, the result is a voltage collapse of the system, which is also observed if the contingency depicted in this figure occurs at the operating point associated with P_L = 0.6 p.u. The maximum loading points correspond in this case to a maximum limit on the generator reactive power Q_G, with the Jacobian of the power flow being nonsingular. This point may be associated with a *limit-induced bifurcation* of a dynamic model of this system (Cañizares, 2002). (A limit-induced bifurcation is defined in a power-flow model of the nonlinear power grid as a point at which 2 power-flow solutions merge as the load is increased; the Jacobian of the power-flow equations at this point is not singular, and corresponds to a power-flow solution where a system controller reaches a control limit, such as a voltage regulating generator reaching a maximum reactive power limit.)

For this simple generator-load example, different PV and QV curves can be computed depending on the system parameters chosen to plot these curves. For example, the family of curves shown in Fig. 11.15 is produced by maintaining the sending end voltage constant while the load at the receiving end is varied at a constant power factor and the receiving end voltage is calculated. Each curve is calculated at a specific power factor and shows the maximum power that can be transferred at this particular power factor, which is also referred to as the maximum system loadability. Note that the limit can be increased by providing more reactive support at the receiving end [limit (2) vs. limit (1)], which is effectively pushing the power factor of the load in the leading direction. It should also be noted that the points on the curves below the limit line V_s characterize unstable behavior of the system where a drop in demand is associated with a drop in the receiving end voltage, leading to eventual collapse. Proximity to voltage instability is usually measured by the distance (in p.u. power) between the operating point on the PV curve and the limit of the same curve; this is usually referred to as the system loadability margin.

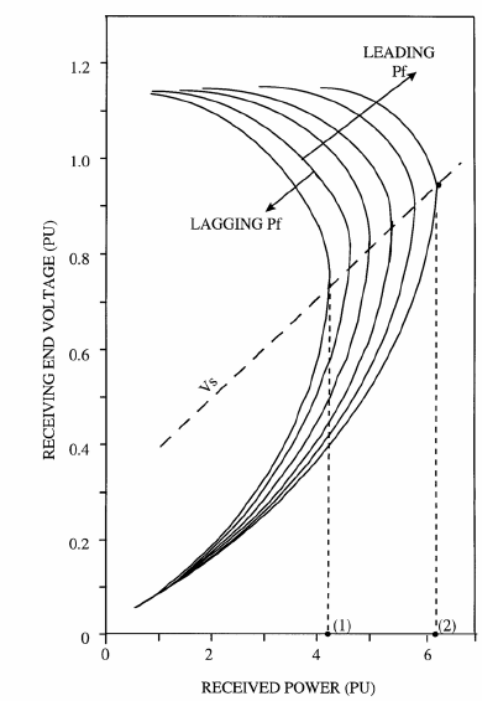

FIGURE 11.15 P_L-V_2 characteristics.

Another family of curves similar to that of Fig. 11.16 can be produced by varying the reactive power demand (or injection) at the receiving end while maintaining the real power and the sending end voltage constant. The relation between the receiving end voltage and the reactive power injection at the receiving end is plotted to produce the so called QV curves of Fig. 11.16. The bottom of any given curve characterizes the voltage stability limit. Note that the behavior of the system on the right side of the limit is such that an increase in reactive power injection at the receiving end results in a receiving end voltage rise, while the opposite is true on the left side because of the substantial increase in current at the lower voltage, which, in turn, increases reactive losses in the network substantially. The proximity to voltage instability or voltage stability margin is measured as the difference between the reactive power injection corresponding to the operating point and the bottom of the curve. As the active power transfer increases (upwards in Fig. 11.16), the reactive power margin decreases, as does the receiving end voltage.

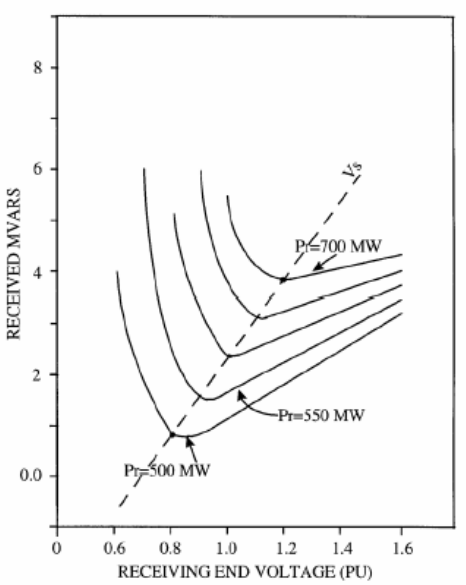

FIGURE 11.16 Q_L-V_2 characteristics.

Load Modeling

Voltage instability is typically associated with relatively slow variations in network and load characteristics. Network response in this case is highly influenced by the slow-acting control devices such as transformer on-load tap changers or LTCs, automatic generation control, generator field current limiters, generator overload reactive capability, under-voltage load shedding relays, and switchable reactive devices. Load characteristics with respect to changing voltages play also a mayor role in voltage stability. The characteristics of such devices as to how they influence the network response to voltage variations are generally understood and well-covered in the literature.

While it might be possible to identify the voltage response characteristics of a large variety of individual equipment of which a power network load is comprised, it is not practical or realistic to model network load by individual equipment models. Thus, the aggregate load model approach is much more realistic. However, load aggregation requires making certain assumptions, which might lead to significant differences between the observed and simulated system behavior. It is for these reasons that load modeling in voltage stability studies, as in any other kind of stability study, is a rather important and difficult issue.

Field test results as reported by Hill (1992) and Xu et al. (1996) indicate that typical response of an aggregate load to step-voltage changes is of the form shown in Fig. 11.17. The response is a reflection of the collective effects of all downstream components ranging from LTCs to individual household loads. The time span for a load to recover to steady-state is normally in the range of several seconds to minutes, depending on the load composition. Responses for real and reactive power are qualitatively similar. It can be seen that a sudden voltage change causes an instantaneous power demand change. This change defines the transient characteristics of the load and was used to derive static load models for angular stability studies. When the load response reaches steady state, the steady-state power demand is a function of the steady-state voltage. This function defines

the steady-state load characteristics known as voltage-dependent load models in power flow studies.

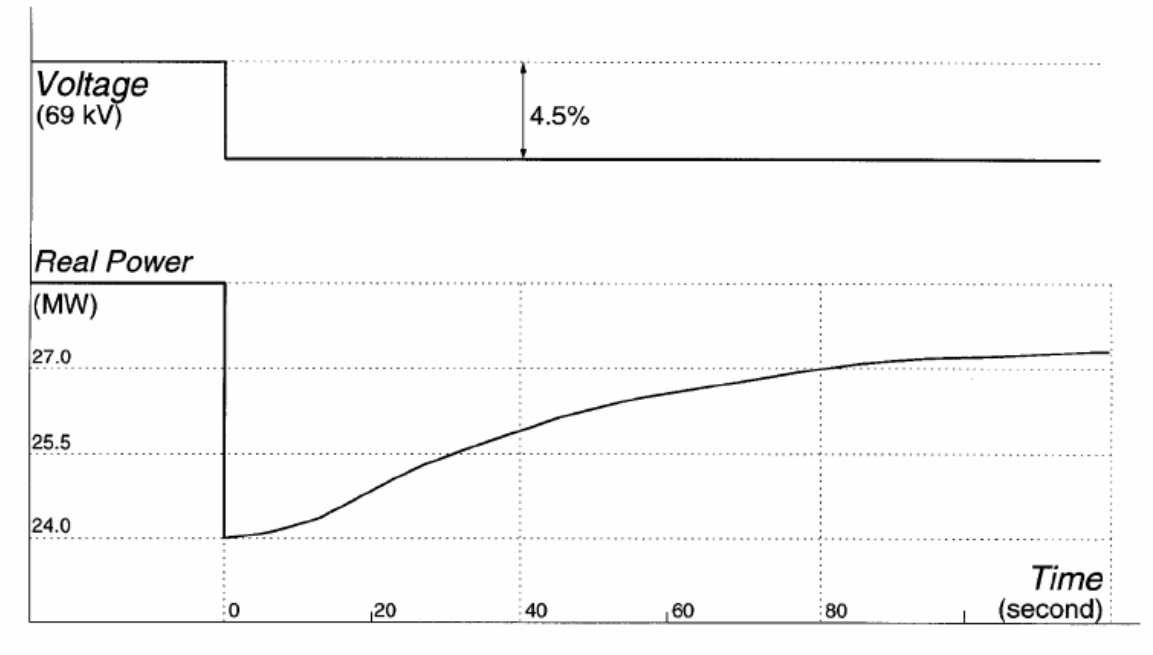

FIGURE 11.17 Aggregate load response to a step voltage change.

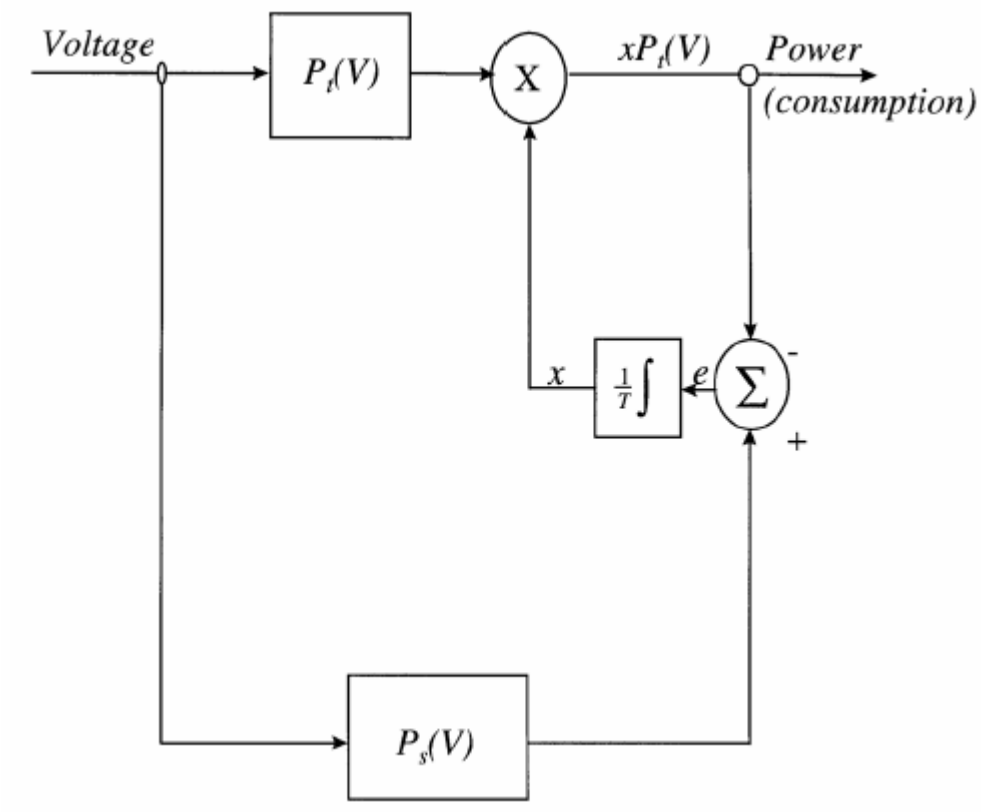

FIGURE 11.18 A generic dynamic load model.

The typical load-voltage response characteristics can be modeled by a generic dynamic load model proposed in Fig. 11.18. In this model (Xu et al., 1993), x is the state variable. $P_t(V)$ and $P_s(V)$ are the transient and steady-state load characteristics, respectively, and can be expressed as:

$$P_t = V^a \quad \text{or} \quad P_t = C_2V^2 + C_1V + C_o$$

$$P_s = P_oV^a \quad \text{or} \quad P_s = P_o\left(d_2V^2 + d_1V + d_o\right)$$

where V is the p.u. unit magnitude of the voltage imposed on the load. It can be seen that, at steady-state, the state variable x of the model is constant. The input to the integration block, $E = Ps - P$, must be zero and, as a result, the model output is determined by the steady-state characteristics $P = Ps$. For any sudden voltage change, x maintains its predisturbance value initially, because the integration block cannot change its output instantaneously. The transient output is then determined by the transient characteristics $P - x\,P_t$. The mismatch between the model output and the steady-state load demand is the error signal e. This signal is fed back to the integration block that gradually changes the state variable x. This process continues until a new steady-state ($e = 0$) is reached. Analytical expressions of the load model, including real (P) and reactive (Q) power dynamics, are:

$$T_p\frac{dx}{dt} = P_s\left(V\right) - P, P = xP_t\left(V\right)$$

$$T_q\frac{dy}{dt} = Q_s\left(V\right) - Q, Q = yQ_t\left(V\right)$$

$$P_t\left(V\right) = V^a, P_s\left(V\right) = P_oV^a; \quad Q_s\left(V\right) = V^\beta, Q_s\left(V\right) = Q_oV^\beta$$

Effect of Load Dynamics on Voltage Stability

As illustrated with the help of the aforementioned generator-load example, voltage stability may occur when a power system experiences a large disturbance such as a transmission line outage. It may also occur if there is no major disturbance but the system's operating point shifts slowly towards stability limits. Therefore, the voltage stability problem, as other stability problems, must be investigated from two perspectives, the large-disturbance stability and the small-signal stability.

Large-disturbance voltage stability is event-oriented and addresses problems such as postcontingency margin requirement and response of reactive power support. Small-signal voltage stability investigates the stability of an operating point. It can provide such information as to the areas vulnerable to voltage collapse. In this section, the effect of load dynamics on large and small disturbance voltage stability is analyzed by examining the interaction of a load center with its supply network, and key parameters influencing voltage stability are identified. Since the real power dynamic behavior of an aggregate load is similar to its reactive power counterpart, the analysis is limited to reactive power only.

Large-Disturbance Voltage Stability

To facilitate the explanation, assume that the voltage dynamics in the supply network are fast as compared to the aggregate dynamics of the load center. The network can then be modeled by three quasi-steady-state V–Q characteristics (QV curves), predisturbance, postdisturbance and postdisturbance-with-reactive-support, as shown in Fig. 11.19. The load center is represented by a generic dynamic load. This load-network system initially operates at the intersection of the steady-state load characteristics and the predisturbance network V–Q curve, point a.

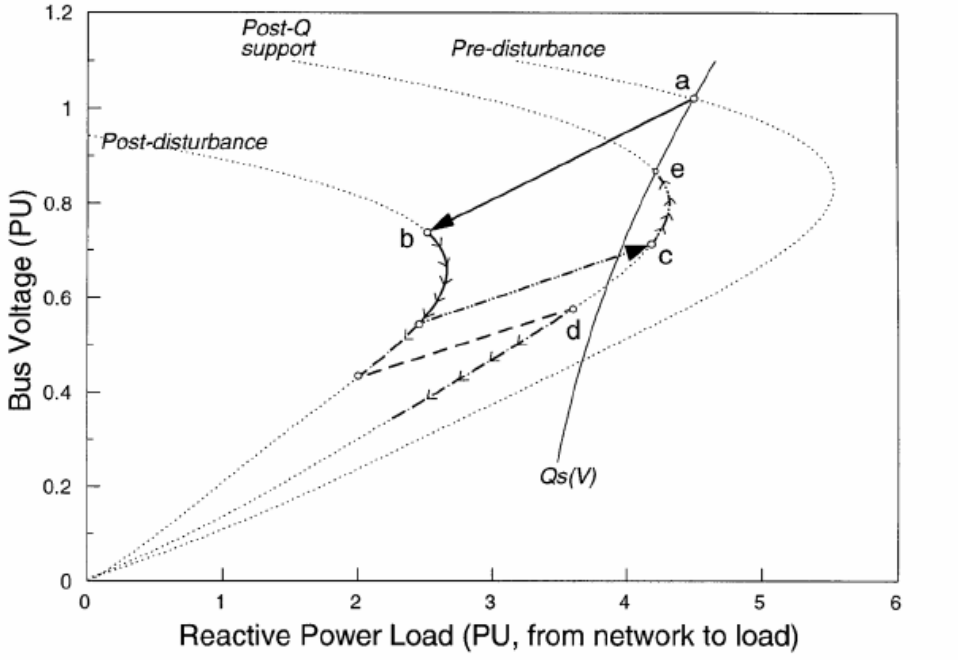

FIGURE 11.19 Voltage dynamics as viewed from V-Q plane.

The network experiences an outage that reduces its reactive power supply capability to the postdisturbance V–Q curve. The aggregate load responds (see section on Load Modeling) instantaneously with its transient characteristics ($\beta = 2$, constant impedance in this example) and the system operating point jumps to point b. Since, at point b, the network reactive power supply is less than load demand for the given voltage:

$$T_q \frac{dy}{dt} = Q_s(V) - Q(V) > 0$$

the load dynamics will try to draw more reactive power by increasing the state variable y. This is equivalent to increasing the load admittance if $\beta = 2$, or the load current if $\beta = 1$. It drives the operating point to a lower voltage. If the load demand and the network supply imbalance persist, the system will continuously operate on the intersection of the postdisturbance V–Q curve and the drifting transient load curve with a monotonically decreasing voltage, leading to voltage collapse.

If reactive power support is initiated shortly after the outage, the network is switched to the third V–Q curve. The load responds with its transient characteristics and a new operating point is formed. Depending on the switch time of reactive power support, the

new operating point can be either c, for fast response, or d, for slow response. At point c, power supply is greater than load demand ($Q_s(V) - Q(V) < 0$); the load then draws less power by decreasing its state variable, and as a result, the operating voltage is increased. This dynamic process continues until the power imbalance is reduced to zero, namely a new steady-state operating point is reached (point e). On the other hand, for the case with slow response reactive support, the load demand is always greater than the network supply. A monotonic voltage collapse is the ultimate end.

A numerical solution technique can be used to simulate the above process. The equations for the simulation are:

$$T_q \frac{dy}{dt} = Q_s(V) = Q(t): \quad Q(t) = yQ_t(V)$$

$$Q(t) = Network(V_s t)$$

where the function $Network(V_s t)$ consists of three polynomials each representing one V–Q curve. Figure 11.19 shows the simulation results in V–Q coordinates. The load voltage as a function of time is plotted in Fig. 11.20. The results demonstrate the importance of load dynamics for explaining the voltage stability problem.

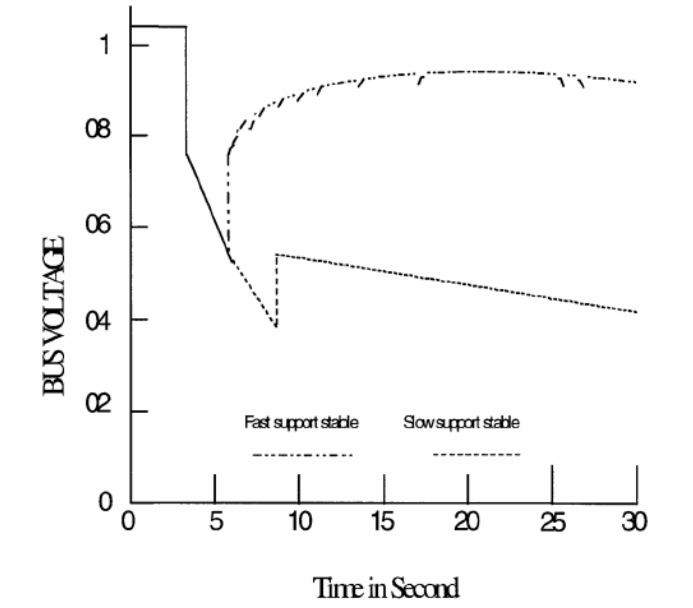

FIGURE 11.20 Simulation of voltage collapse.

Small-Signal Voltage Stability

The voltage characteristics of a power system can be analyzed around an operating point by linearizing the power flow equations around the operating point and analyzing the resulting sensitivity matrices. Breakthroughs in computational algorithms have made these techniques efficient and helpful in analyzing large-scale systems, taking into account virtually all the important elements affecting the phenomenon. In particular, singular value decomposition and modal techniques should be of particular interest to the reader and are thoroughly described by Mansour (1993), Lof et al. (1992 and 993), Gao et al. (1992), and Cañizares (2002).

Analytical Framework

The slow nature of the network and load response associated with the phenomenon makes it possible to analyze the problem in two frameworks: (1) long-term dynamic framework in which all slow-acting devices and aggregate bus loads are represented by their dynamic models (the analysis in this case is done through a dynamic o quasy-dynamic simulation of the system response to contingencies or load variations), or (2) steady-state framework (e.g. power flow) to determine if the system can reach a stable operating point following a particular contingency. This operating point could be a final state or a midpoint following a step of a discrete control action (e.g. transformer tap change).

The proximity of a given system to voltage instability and the control actions that may be taken to avoid voltage collapse are typically assessed by various indices and sensitivities. The most widely used are (Cañizares, 2002):

- Loadability margins, i.e. the "distance" in MW or MVA to a point of voltage collapse, and sensitivities of these margins with respect to a variety of parameters, such as active/reactive power load variations or reactive power levels at different sources.
- Singular values of the system Jacobian or other matrices obtained from these Jacobians, and their sensitivities with respect to various system parameters,
- Bus voltage profiles and their sensitivity to variations in active and reactive power of the load and generators, or other reactive power sources.
- Availability of reactive power supplied by generators, synchronous condensers and static-var compensators and its sensitivity to variations in load bus active and/or reactive power.

These indices and sensitivities, as well as their associated control actions, can be determined using a variety of the computational methods described below.

Power Flow Analysis

Partial PV and QV curves can be readily calculated using power flow programs. In this case, the demand of load center buses is increased in steps at a constant power factor while the generators' terminal voltages are held at their nominal value, as long as their reactive power outputs are within limits; if a generator reactive power limits is reached, the corresponding generator bus is treated as another load bus. The PV relation can then be plotted by recording the MW demand level against a "central" load bus voltage at the load center. It should be noted that power flow solution algorithms diverge very close to or past the maximum loading point, and do not produce the unstable portion of the PV relation. The QV relation, however, can be produced in full by assuming a fictitious synchronous condenser at a central load bus in the load center (this is a "parameterization" technique also used in the continuation methods described below). The QV relation is then plotted for this particular bus as a representative of the load center by varying the voltage of the bus (now converted to a voltage control bus by the addition of the synchronous condenser) and recording its value against the reactive power injection of the synchronous condenser. If the limits on the reactive power capability of

the synchronous condenser are made very high, the power flow solution algorithm will always converge at either side of the QV relation.

Continuation Methods

A popular and robust technique to obtain full PV and/or QV curves is the continuation method (Cañizares, 2002). This methodology basically consists of two power-flow-based steps: the predictor and the corrector, as illustrated in Fig. 11.21. In the predictor step, an estimate of the power flow solution for a load P increase (point 2 in Fig. 11.21) is determine based on the starting solution (point 1) and an estimate of the changes in the power flow variables (e.g. bus voltages and angles). This estimate may be computed using a linearization of the power flow equations, i.e. determining the "tangent vector" to the manifold of power flow solutions. Thus, in the example depicted in Fig. 11.21:

$$\begin{aligned} \Delta x &= x_2 - x_1 \\ &= k\, J_{PF_1}^{-1} \left.\frac{\partial f_{PF}}{\partial P}\right|_1 \Delta P \end{aligned}$$

where J_{PF1} is the Jacobian of the power flow equations $f_{PF}(x) = 0$, evaluated at the operating point 1; x is the vector of power flow variables (load bus voltages are part of x); $\partial\, f_{PF}/\partial\, P|_1$ is the partial derivative of the power flow equations with respect to the changing parameter P evaluated at the operating point 1; and k is an constant used to control the length of the step (typically $k = 1$), which is usually reduced by halves to guarantee a solution of the corrector step near the maximum loading point, and thus avoid the need for a parameterization step. Observe that the predictor step basically consist on determining the sensitivities of the power flow variables x with respect to changes in the loading level P.

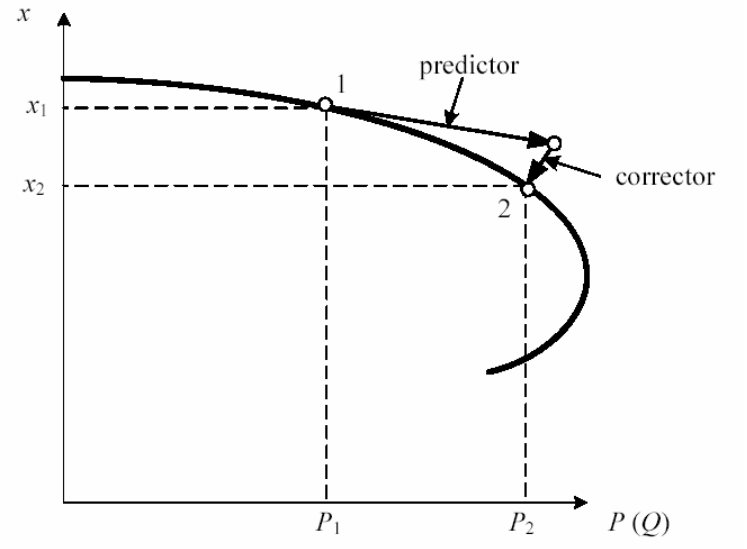

FIGURE 11.21 Continuation power flow.

The corrector step can be as simple as solving the power flow equations for $P = P_2$ to obtain the operating point 2 in Fig. 11.21, using the estimated values of x yielded by the predictor as initial guesses. Other more sophisticated and computationally robust techniques, such as a "perpendicular intersection" method, may be used as well.

Optimization or Direct Methods

The maximum loading point can be directly computed using optimization-based methodologies (Rosehart, 2002), which yield the maximum loading margin to a voltage collapse point and a variety of sensitivities of the power flow variables with respect to any system parameter, including the loading levels (Milano, 2005). These methods basically consist on solving the optimal power flow (OPF) problem:

$$\begin{aligned} \text{Max.} \quad & P \\ \text{s.t.} \quad & f_{PF}(x, P) = 0 \ \rightarrow \ \text{power flow eqs.} \\ & x_{min} \leq x \leq x_{max} \ \rightarrow \ \text{limits} \end{aligned}$$

where P represents the system loading level; the power flow equations f_{PF} and variable x should include the reactive power flow equations of the generators, so that the generator's reactive power limits can be considered in the computation. The Lagrange multipliers associated with the constraints are basically sensitivities that can be used for further analyses or control purposes. Well-known optimization techniques, such as Interior Point methods, can be used to obtain loadability margins and sensitivities by solving this particular OPF problem for real-sized systems.

Approaching voltage stability analysis from the optimization point of view has the advantage that certain variables, such as generator bus voltages or active power outputs, can be treated as optimization parameters. This allows treating the problem not only as a voltage stability margin computation, but also as a means to obtain an "optimal" dispatch to maximize the voltage stability margins.

Time scale decomposition

The PV and QV relations produced results corresponding to an end state of the system where all tap changers and control actions have taken place in time and the load characteristics were restored to a constant power characteristic. It is always recommended and often common to analyze the system behavior in its transition following a disturbance to the end state. Aside from the full long-term time simulation, the system performance can be analyzed in a quasidynamic manner by breaking the system response down into several time windows, each of which is characterized by the states of the various controllers and the load recovery (Mansour, 1993). Each time window can be analyzed using power flow programs modified to reflect the various controllers' states and load characteristics. Those time windows (Fig. 11.21) are primarily characterized by:

1. Voltage excursion in the first second after a contingency as motors slow, generator voltage regulators respond, etc.
2. The period 1 to 20 sec when the system is quiescent until excitation limiting occurs

3. The period 20 to 60 sec when generator over excitation protection has operated
4. The period 1 to 10 min after the disturbance when LTCs restore customer load and further increase reactive demand on generators
5. The period beyond 10 min when AGC, phase angle regulators, operators, etc. come into play

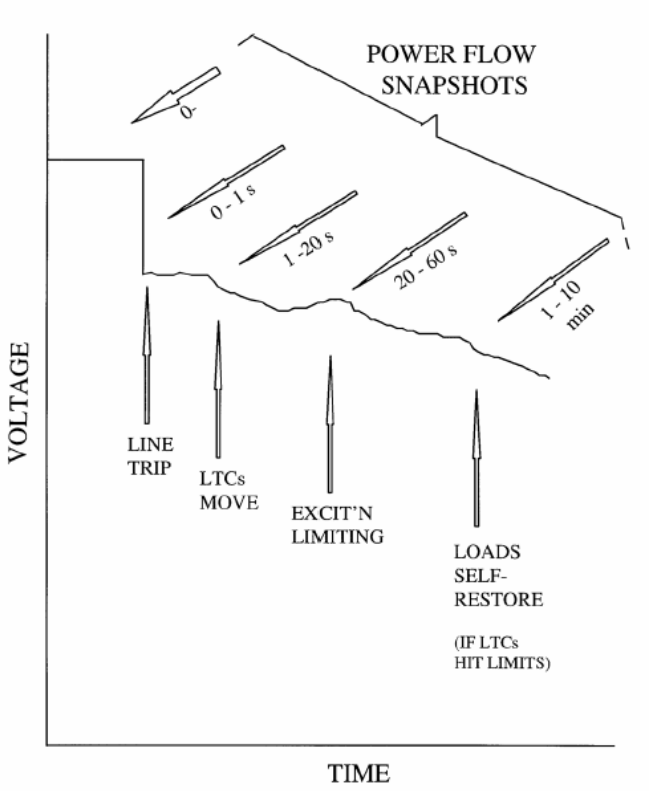

FIGURE 11.21 Breaking the system response down into time periods.

The sequential power flow analysis aforementioned can be extended further by properly representing in the simulation some of the slow system dynamics, such as the LTCs' (Van Cutsem, 1996).

Mitigation of Voltage Stability Problems

The following methods can be used to mitigate voltage stability problems.

Must-Run Generation. Operate uneconomic generators to change power flows or provide voltage support during emergencies or when new lines or transformers are delayed.

Series Capacitors. Use series capacitors to effectively shorten long lines, thus decreasing the net reactive loss. In addition, the line can deliver more reactive power from a strong system at one end to one experiencing a reactive shortage at the other end.

Shunt Capacitors. Though the heavy use of shunt capacitors can be part of the voltage stability problem, sometimes additional capacitors can also solve the problem by freeing "spinning reactive reserve" in generators. In general, most of the required reactive power should be supplied locally, with generators supplying primarily active power.

Static Compensators (SVCs and STATCOMs). Static compensators, the power electronics-based counterpart to the synchronous condenser, are effective in controlling voltage and preventing voltage collapse, but have very definite limitations that must be recognized. Voltage collapse is likely in systems heavily dependent on static compensators when a disturbance exceeding planning criteria takes these compensators to their ceiling.

Operate at Higher Voltages. Operating at higher voltage may not increase reactive reserves, but does decrease reactive demand. As such, it can help keep generators away from reactive power limits, and thus help operators maintain control of voltage. The comparison of receiving end Q–V curves for two sending end voltages shows the value of higher voltages.

Secondary Voltage Regulation. Automatic voltage regulation of certain load buses, usually referred to as pilot buses, that coordinately controls the total reactive power capability of the reactive power sources in pilot buses' areas, has proven to be an effective way to improve voltage stability (Cañizares, 2005). These are basically hierarchical controls that directly vary the voltage set points of generators and static compensators on a pilot bus' control area, so that all controllable reactive power sources are coordinated to adequately manage the reactive power capability in the area, keeping some of these sources from reaching their limits at relatively low load levels.

Undervoltage Load Shedding. A small load reduction, even 5 to 10%, can make the difference between collapse and survival. Manual load shedding is used today for this purpose (some utilities use distribution voltage reduction via SCADA), though it may be too slow to be effective in the case of a severe reactive shortage. Inverse time-undervoltage relays are not widely used, but can be very effective. In a radial load situation, load shedding should be based on primary side voltage. In a steady-state stability problem, the load shed in the receiving system will be most effective, even though voltages may be lowest near the electrical center (shedding load in the vicinity of the lowest voltage may be more easily accomplished, and still be helpful).

Lower Power Factor Generators. Where new generation is close enough to reactive-short areas or areas that may occasionally demand large reactive reserves, a .80 or .85 power factor generator may sometimes be appropriate. However, shunt capacitors with a higher power factor generator having reactive overload capability may be more flexible and economic.

Use Generator Reactive Overload Capability. Generators should be used as effectively as possible. Overload capability of generators and exciters may be used to delay voltage collapse until operators can change dispatch or curtail load when reactive overloads are modest. To be most useful, reactive overload capability must be defined in advance, operators trained in its use, and protective devices set so as not to prevent its use.

References

Cañizares, C. A., editor, *Voltage Stability Assessment: Concepts, Practices and Tools*, IEEE-PES Power Systems Stability Subcommittee Special Publication, SP101PSS, August, 2002.

Cañizares, C. A., Cavallo, C., Pozzi, M., Corsi, S., Comparing Secondary Voltage Regulation and Shunt Compensation for Improving Voltage Stability and Transfer Capability in the Italian Power System, *Electric Power Systems Research*, 73, 67–76, January, 2005.

Gao, B., Morison, G.K., Kundur, P., Voltage Stability Evaluation Using Modal Analysis, *IEEE Trans. on Power Systems*, 7, 1529–1542, November, 1992.

Hill, D. J., Nonlinear Dynamic Load Models with Recovery for Voltage Stability Studies, *IEEE Trans. on Power Systems*, 8, 166–176, February, 1993.

IEEE-CIGRE Joint Task Force on Stability Terms and Definitions (Kundur, P., Paserba, J., Ajjarapu, V., Andersson, G., Bose, A., Cañizares, C., Hatziargyriou, N., Hill, D., Stankovic, A., Taylor, C., Van Cutsem, T., Vittal, V.), Definition and Classification of Power System Stability, *IEEE Trans. on Power Systems*, 19, 1387–1401, August, 2004.

Lof, P.-A., Andersson, G., Hill, D. J., Voltage Stability Indices for Stressed Power Systems, *IEEE Trans. on Power Systems*, 8, 326–335, February, 1993.

Lof, P.-A., Smed, T., Andersson, G., Hill, D.J., Fast Calculation of a Voltage Stability Index, *IEEE Trans. on Power Systems*, 7, 54–64, February, 1992.

Mansour, Y., Editor, *Suggested Techniques for Voltage Stability Analysis*, IEEE Special Publication #93TH0620-5-PWR, 1993.

Mansour, Y., Editor, *Voltage Stability of Power Systems: Concepts, Analytical Tools, and Industry Experience*, IEEE Special Publication # 90TH0358-2-PWR, 1990.

Milano, F., Cañizares, C. A., Conejo, A. J., Sensitivity-based Security-constrained OPF Market Clearing Model, to appear in *IEEE Trans. on Power Systems*, 2006.

Rosehart, W, Cañizares, C. A., Quintana, V, Multi-objective Optimal Power Flows to Evaluate Voltage Security Costs, *IEEE Trans. on Power Systems*, 18, 578–587, May, 2003.

US-Canada Power System Outage Task Force, *Final Report on the August 14, 2003 Blackout in the United States and Canada: Causes and Recommendations*, April, 2004.

Van Cutsem, T., Vournas, C.D., Voltage Stability Analysis in Transient and Midterm Time Scales, *IEEE Tran. on Power Systems*, 11, 146–154, February, 1996.

Venikov, V., *Transient Processes in Electrical Power Systems*, Mir Publishers, Moscow, 1970 and 1980.

Xu, W., Mansour, Y., Voltage Stability Analysis Using Generic Dynamic Load Models, *IEEE Trans. on Power Systems*, 9, 479–493, February, 1994.

Xu, W., Vaahedi, E., Mansour, Y., Tamby, J., Voltage Stability Load Parameter Determination from Field Tests on B. C. Hydro's System, *IEEE Trans. on Power Systems*, 12, 1290–1297, August, 1997.